# An Efficient Geometry-Induced Genetic Algorithm for Base Station Placement in Cellular Networks

**YAXI LIU**[1], (Student Member, IEEE), **WEI HUANGFU**[1], (Member, IEEE),
**HAIJUN ZHANG**[1], (Senior Member, IEEE), **HAOBIN WANG**[1,2], **WEI AN**[1],
**AND KEPING LONG**[1], (Senior Member, IEEE)

[1]Beijing Advanced Innovation Center for Materials Genome Engineering, Beijing Engineering and Technology Research Center for Convergence Networks and Ubiquitous Services, School of Computer and Communication Engineering, University of Science and Technology Beijing, Beijing 100083, China
[2]China Telecom Beijing Research Institute, China Telecom Company Ltd., Beijing 102209, China

Corresponding author: Wei Huangfu (huangfuwei@ustb.edu.cn)

**ABSTRACT** During the phase of the Base Station (BS) deployment, the BS placement, as an essential issue in achieving seamless coverage of the existing, even the future version of cellular networks, should be attached extensive attention. The ignorance of the geometric distribution of the candidate sites results in negative impact on the performance of traditional meta-heuristic algorithms related to the base station placement problem. A novel geometry-induced genetic algorithm is proposed as an efficient solution to the problem based on both the local coverage evaluation and the local geometric site pattern reservation. The deployment region is divided into sub-regions and the site assignment in the sub-regions is encoded to geometry-aware chromosome segment, which reflects the geometric correlation among the BSs. In the crossover operation, the segments of the chromosomes, while representing the sites inside a sub-region, are exchanged as a whole. In the mutation operation, the overall coverage performance witnesses improvement with the gradual decoration of the poor sub-regions. The experiments for both the ideal disk coverage model and the real radio signal coverage model are executed. The results prove the validity and the efficiency of the proposed algorithms.

**INDEX TERMS** Wireless cellular networks, base station placement problem, coverage, geometry-induced, genetic algorithm.

## I. INTRODUCTION

In the last decade, the popularization of the smart handheld wireless devices leads to the tremendous growth of service flow in wireless cellular networks, which requires qualified Quality of Service (QoS) anytime and anywhere [1]. Among the metrics of QoS, coverage is important to be evaluated by the network operators [2], [3]. During the phase of the Base Station (BS) deployment, the BS placement problem occurs as a determinant optimization issue for maximizing coverage in the generations of mobile networks [4]–[6].

The BS placement problem involves determining a subset of locations to deploy the BSs from a set of candidate sites. The locations of the candidate sites are usually constrained

by factors such as the practical terrain [7], [8]. The geometric distribution models of the BSs, as well as the corresponding metrics, have been discussed [9]. The BS placement problem is proved to be a combinatorial optimization problem, or more precisely, a typical Non-deterministic Polynomial-time (NP)-hard problem [10]. The computational complexity of such problems increases sharply along with the growth of candidate sites number. And it is harder to improve the efficiency of BSs. [11]–[14]. Therefore, it is essential for mobile network operators to invent more money in sufficient algorithms, so as to handle the BS placement problem within a limited time.

The existing algorithms for handling the BS placement problem can be roughly classified into three categories: the exact approaches, the heuristic ones and the meta-heuristic ones. The exact approaches usually obtain the global optimal solution by exhaustive searching or global searching

The associate editor coordinating the review of this manuscript and approving it for publication was Emrecan Demirors.

methods at the cost of inefficiency. In order to decrease the computational complexity, researchers have proposed algorithms with heuristic techniques to obtain a near-optimum or a satisfactory solution. The heuristic algorithms are usually problem-oriented whereas the meta-heuristic ones are problem-independent. The latter thus attracts more attention. Among the existing meta-heuristic algorithms, GA (Genetic Algorithm) is a typical approach to handle the aforementioned BS placement problems [15]–[18].

Note that the crossover and the mutation operations in the canonical GA are problem-independent, resulting in the ignorance of the geometric distribution of the BSs. Therefore, it will deteriorate the performance of the algorithm. The reason is mainly two-folds.

Firstly, in a given sub-region where a certain subset of sites is chosen for deploying BSs, the coverage ratio related to this sub-region mainly depends upon the BSs inside it. Theoretically, such a locality property means that the chromosome is possible to be evaluated in a local manner, nor in a global manner. It will inspire us how to design the mutation and the crossover operators on a limited range of the chromosome by the locality evaluation.

Secondly, the geometric pattern of the sites chosen for a given sub-region should be reasonable and well-distributed to yield a good coverage ratio. Thus, the geometric pattern of these BSs is rather important as a whole. Although the sites chosen are possibly modified to better the coverage ratio, a good geometric pattern of the BSs, as a whole, should be inherited from the previous generation, which can be named as locality reservation.

However, to the best of our knowledge, neither the locality evaluation of the coverage ratio nor the locality reservation of the geometric distribution of the sites is explicitly considered in the existing approaches to the BS placement problems.

Inspired by the aforementioned geometric characteristics of the BSs, we take advantage of the local coverage evaluation and local geometric pattern reservation, so as to further boost the convergence speed of the GA algorithm. In this paper, we propose a novel Geometry-induced Genetic Algorithm (GGA) to handle the BS placement problems in cellular networks. We divide the ROI (Region of Interest) into sub-regions and thus decompose the original optimization objective related to the whole service region into sub-objectives related to the sub-regions. For an individual in the GA, i.e., a given feasible solution representing a combination of the BS candidate sites, we take into account not only the coverage ratio value related to the whole ROI, but also the local coverage ratio values related to the sub-regions. For a given sub-region, a higher local coverage ratio indicates a better performance of the genes corresponding to the sub-region in the chromosome of the individual. Thus, we can determinate where the coverage is not qualified and which segments of the chromosome should be improved. In the mutation operation, we consciously revise the genes in chromosome segment where the local coverage fitness functions are low instead of uniformly random revising, which

indirectly improves the overall performance by utilizing the geometric guidance. In the crossover operation, we exchange the genes related to the same sub-region of two individuals, which ensures that the site pattern of the corresponding sub-region is inherited. Finally we testify the feasibility and the efficiency of the proposed GGA with experiments.

The rest of the paper is organized as follows. Section II discusses the related work. Section III introduces the system model and formulates the problem. Section IV proposes the GGA algorithm. Section V and section VI present the experiments and discusses the results. Finally, Section VII concludes this paper.

## II. RELATED WORK

Exact approaches usually utilize the mathematical modeling or the exhaustive searching to select the global optimal solution to the BS placement problems. Wright [19] proposed a customized variant of the Nelder-Mead simplex method to find the optimal BS placement. Radmard *et al.* [20] used the exhaustive method to place the transmitters. Although the result of such approach is theoretically globally optimal, the computational efficiency is low for large-scale problems. Usually, a near-optimal solution is enough and it is unnecessary to obtain the global optimum at the expense of the computation time.

In order to balance the accuracy and the efficiency, researchers have proposed some heuristic algorithms to obtain a satisfactory solution within a limited time. Abdelkhalek *et al.* [21] adopted a new Multi-Objective Variable Neighborhood Search algorithm to automatically select the most promising neighborhood. Bi and Zhang [22] utilized the greedy algorithm to minimize the system cost with satisfied energy harvesting and communication performance for node placement optimization. Lagum *et al.* [23] proposed a greedy-type heuristic algorithm based on the Voronoi diagram in unmanned aerial vehicle BSs' horizontal placement problems.

Different from the heuristic algorithms, the meta-heuristic algorithms which do not utilize the particularity of the problems are problem-independent. Meta-heuristic algorithms can be further classified into continuous meta-heuristic algorithms, which are designed to cope with the continuous solution space, and discrete meta-heuristic algorithms, which are designed to operate the discrete one. Typical continuous meta-heuristic algorithms include Particle Swarm Optimization (PSO) algorithm, the Bee Colony (BC) algorithm, the Cuckoo Search (CS) algorithm, the Simulated Annealing (SA) algorithm and Tabu Search (TS) algorithm. Indeed, despite the fact that the continuous meta-heuristic algorithms are only feasible for continuous optimization problems, many researchers have improved them to further deal with the discrete ones, such as the binary PSO algorithm [24], the binary artificial BC algorithm [25], the binary CS algorithm [26], etc. However, such improved algorithms makes the problem more complex, further affecting algorithm's efficiency and sensitivity.

As one of the most common meta-heuristic algorithms The genetic algorithms are successfully used for handling the BS placement problems. According to the number of the optimization objectives, the GAs can be classified into single-objective GAs and multi-objective GAs. Al-Samawi *et al.* [27] presented a single-objective GA to estimate the best sites for BSs with one objective, i.e., BS power efficiency. For some multi-objective GAs, the fitness functions can be obtained by simply summing all objectives or allocating weight for each objective, and then the multi-objective GAs are degraded into the single-objective GAs. Huang *et al.* [28] designed a multi-objective GA with four objectives, namely, the area coverage, the traffic capacity, the interference level and the system cost, and defined the fitness function as the summation of them. Hu and Goodman [29] provided a multi-objective GA of which the fitness function was the summation of the artificially weighted objectives. Munyaneza *et al.* [30] also used the summation of the weighted objectives to conduct the multi-objective GA. The other multi-objective GAs are originally designed to deal with the optimization problems with more than one fitness functions. Raisanen and Whitaker [31] considered four multi-objective GAs, namely, the Strength Pareto Evolutionary Algorithm version II (SPEA2), the Non-dominated Sorting Genetic Algorithm version II (NSGA-II), the Pareto Envelope-based Selection Algorithm (PESA) and the Simple Evolutionary Algorithm for Multi-objective Optimization (SEAMO), to select and configure BS sites for the BS placement problems. Ting *et al.* [32] determined the sites of heterogeneous transmitters by considering four fitness functions, namely, the coverage, the cost, the capacity and the overlap, and adopted NSGA-II to handle the BS placement problems. Abdelkhalek *et al.* [33] applied the Variable-Length Genetic Algorithm (VLGA) to handle an BS placement problem with 20 constraints and objectives.

According to the coding methods, GAs can be classified into binary-coding GAs, real-coding GAs and probability-coding GAs. Maple *et al.* [34] presented a parallel genetic algorithm to obtain the optimum BS placement and denoted a gene as the selected state of a candidate site. If the candidate site was selected, the gene was 1. Otherwise, the gene was 0. Han *et al.* [35] described the BS placement with the real coordinate number, and thus the length of an individual was as twice as the the number of selected BS sites. Wang *et al.* [36] used the polar radii and the polar angles of BSs to conduct the real-coding GA. Yang *et al.* [37] employed the lists of the sequence numbers of the selected sites to express the individuals. Dahi *et al.* [38] proposed a Quantum-Inspired Genetic Algorithm (QIGA) for the BS placement problems, and the gene of candidate site was represented by the probability of being selected and the probability of not being selected. However, the existing GAs for handling the BS placement problems mainly neglect the geometric correlation among the adjacent BSs. Usually, a gene represents the state whether a candidate site is selected and thus the sequence of the genes is not relevant to the geometric locations of BSs.

## III. SYSTEM MODELING AND PROBLEM FORMULATION

Suppose that there are $n$ BS candidate sites, denoted as $S_1, S_2, \ldots, S_n$, in a predefined service region $R$. Among them, there will be $m$ candidate sites chosen to be installed a BS.

Let $\boldsymbol{\alpha} = \{\alpha_1, \alpha_2, \ldots, \alpha_n\}$ denote the site assignment set where $\alpha_i$ indicates whether the candidate $S_i$ is chosen to install the BSs, given by

$$\alpha_i = \begin{cases} 1 & \text{if } S_i \text{ is selected,} \\ 0 & \text{otherwise.} \end{cases} \tag{1}$$

where $\sum_{i=1}^{n} \alpha_i = m \leq n$.

Let the subset of the sites to deploy the BSs be $\hat{\mathbf{S}} = \{\hat{S}_1, \hat{S}_2, \ldots, \hat{S}_m\}$ satisfying

$$\hat{\mathbf{S}} = \{S_i | \alpha_i = 1, 1 \leq i \leq n\}. \tag{2}$$

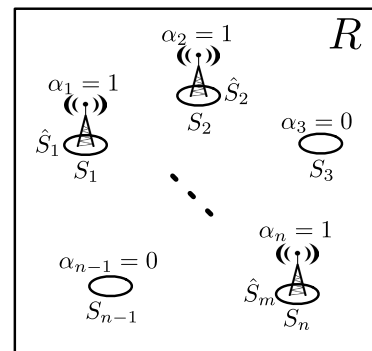The illustration of network deployment is shown in Fig. 1.



**FIGURE 1.** Illustration of the network deployment.

For a given site assignment set $\boldsymbol{\alpha}$, let $c_i(\boldsymbol{\alpha})$ be the covered region of the BS on the candidate site $S_i$ if $\alpha_i = 1$, or let $c_i(\boldsymbol{\alpha}) = \varnothing$ if the candidate site $S_i$ is not selected to place a BS, i.e., $\alpha_i = 0$. A subscriber will access the cellular network via $S_i$ if it is located inside $c_i(\boldsymbol{\alpha})$. Assume that a specific location can only be covered by one BS, and thus the covered regions of all BS sites $c_i$, $1 \leq i \leq n$, are mutually exclusive. Consequently, for arbitrary two candidate sites $S_p$ and $S_q$, $c_p \cap c_q = \varnothing$. Now the coverage area inside the region $R$ can be expressed as

$$Cover(\boldsymbol{\alpha}) = R \cap \left( \sum_{i=1}^{n} c_i(\boldsymbol{\alpha}) \right). \tag{3}$$

Our goal is to maximize the coverage *Cover* by selecting a candidate site subset $\hat{\mathbf{S}}$ from $\mathbf{S}$, i.e., by finding an optimal, or at

least, a near-optimal site assignment set $\boldsymbol{\alpha}$. Thus, the optimization problem can be described as

$$\max_{\boldsymbol{\alpha}} \; Cover(\boldsymbol{\alpha}) = R \cap \left( \sum_{i=1}^{n} c_i(\boldsymbol{\alpha}) \right), \qquad (4)$$

$$\text{s.t. } \alpha_i \in \{0, 1\}, \quad 1 \le i \le n$$

$$\sum_{i=0}^{n} \alpha_i = m.$$

The BS placement problem is proved to be a combinatorial optimization problem [10]. The number of feasible solutions is $C_n^m = \frac{n!}{m!(n-m)!}$. The scale of the solution space is determined by the number of the candidate sites and the number of BSs to be installed.

In order to improve the readability, the notations involved and their meanings are listed in Table 1.

## IV. GEOMETRY-INDUCED GENETIC ALGORITHM

In this section, we divide the region $R$ into sub-regions and further propose a geometry-induced chromosome encoding scheme from a geometric perspective. Then, we present the fitness functions to reflect both the global and the local coverage ratios. Moreover, we introduce the process of the selection operation, the crossover operation and the mutation operation with the geometry-induced chromosome segments.

### A. GENE, GEOMETRY-INDUCED CHROMOSOME, INDIVIDUAL AND POPULATION

Gene is exactly the site assignment indicator representing whether a candidate site is selected to place the BS. Denote the gene set as $\boldsymbol{G} = \{G_1, G_2, \ldots, G_n\}$ where $n$ is the number of the candidate sites and $G_i = \alpha_i$.

To fully exploit the geometric information, we divide the region $R$ into $r$ sub-rectangles. Denote the rectangle set as $\mathbf{R} = \{R_1, R_2, \ldots, R_r\}$. We assume that there are more than one candidate sites located in each rectangle. Thus, the candidate sites, or more precisely, the genes, can be divided into $r$ groups according to the geographic sub-rectangles.

Denote the geometry-induced chromosome segment $C_k$ as a set of genes whose candidate sites are distributed in the region $R_k$, given by

$$C_k = \{G_i | (x_i, y_i) \in R_k\}$$
$$= \left\{ G_1^k, G_2^k, \ldots, G_{n_k}^k \right\} \qquad (5)$$

where $(x_i, y_i)$ is the coordinate of the candidate site $S_i$ and $n_k$ is the number of genes in the region $R_k$. Obviously, the chromosome segments $C_1, C_2, \ldots, C_r$ are mutually exclusive and satisfy

$$C_i \cap C_j = \varnothing, \quad 1 \le i \le n, \; 1 \le j \le n, \; i \ne j \qquad (6)$$
$$C_1 \cup C_2 \cup \ldots \cup C_r = \{G_1, G_2, \ldots, G_n\}. \qquad (7)$$

Note that if $n_k = 1$, $1 \le k \le r$, the $k$-th chromosome segment only contains one gene and the geometric sub-division is meaningless for making use of the correlation among the genes belongs to this sub-region. The illustrations of

**TABLE 1.** Table of notations.

| Symbol | Meaning |
|---|---|
| $n$ | The number of the BS candidate sites |
| $S_i, 1 \le i \le n$ | The $i$-th BS candidate site |
| $\boldsymbol{\alpha}$ | The site assignment set |
| $\alpha_i$ | The $i$-th site assignment indicator |
| $m$ | The number of the BSs prepared to be installed |
| $\hat{\mathbf{S}}$ | Selected BS site subset |
| $\hat{S}_{\hat{i}}, 1 \le \hat{i} \le m$ | The $\hat{i}$-th selected BS site |
| $R$ | Region of interest |
| $c_i$ | Covered region of the BS on site $S_i$ |
| $Cover$ | Coverage inside the region $R$ |
| $\mathbf{G}$ | The gene set |
| $G_i$ | Gene related to $S_i$ |
| $r$ | The number of the sub-rectangles |
| $\mathbf{R}$ | The rectangle set |
| $R_k, 1 \le k \le r$ | The $k$-th sub-rectangle inside $R$ |
| $C_k$ | The chromosome segment related to $R_k$ |
| $n_k$ | The number of the genes in $R_k$ |
| $L$ | The number of the individuals |
| $\mathbf{P}$ | The population |
| $I_l, 1 \le l \le L$ | The $l$-th individual |
| $G_{i_k}^{k,l}, 1 \le i_k \le n_k$ | The $i_k$-th gene of $C_k$ in individual $I_l$ |
| $C_{k,l}$ | The $k$-th chromosome segment of $I_l$ |
| $Cover(C_{k,l})$ | The covered region of $C_{k,l}$ |
| $F_l$ | The fitness function of individual $I_l$ |
| $F_{k,l}$ | The fitness function of $C_{k,l}$ |
| $a$ | Multiplier parameter in fitness function |
| $b$ | Exponent parameter in fitness function |
| $P_{\text{Sel}}^l$ | The selection probability of individual $I_l$ |
| $N_M$ | The number of the chromosome segments selected in the selection operation |
| $P_{\text{Cro}}$ | The crossover probability |
| $P_{\text{Mut}}$ | The mutation probability |
| $P_{\text{Mut}}^{k,l}$ | The mutation probability of $C_{k,l}$ |
| $L_{\text{Ideal}}$ | The length of the region of the interest |
| $r_c$ | The cell coverage radius in ideal disk BS coverage model |
| $|X|$ | The area of the region $X$ |
| $C_{\text{Ratio}}$ | The coverage ratio in region $R$ |
| $D_i(x_i, y_i, r_c)$ | A circle with center $S_i(x_i, y_i)$ and radius $r_c$ |
| $V_i(x_i, y_i)$ | A Voronoi polygons with center $S_i(x_i, y_i)$ |
| $E_{\text{dist}}((x_i, y_i), (x_j, y_j))$ | The Euclidean distance between point $(x_i, y_i)$ and point $(x_j, y_j)$ |
| $P^{\text{RS}}(x, y)$ | The RSRP on coordinate $(x, y)$ |
| $P_j(x, y), 1 \le j \le 3m$ | The signal power on coordinate $(x, y)$ from the $j$-th antenna |
| $P^{\text{SI}}(x, y)$ | The SINR on coordinate $(x, y)$ |
| $Gain_j(x, y)$ | The antenna gain from the $j$-th antenna to coordinate $(x, y)$ |
| $PL_j(x, y)$ | The path loss from the $j$-th antenna to coordinate $(x, y)$ |
| $G_{\text{terminal}}$ | The mobile terminal antenna gain |
| $\sigma_s$ | The shadow fading margin |
| $P_{\text{tx}}$ | The antenna transmit power |
| $\text{TH}_{\text{RS}}$ | The threshold for RSRP |
| $\text{TH}_{\text{SI}}$ | The threshold for sinr |
| $N_{\text{Noise}}$ | Background noise |

the sub-division and the chromosome segments are depicted in Fig. 2.

The individual $I$ refers to the chromosome segment matrix, given by

$$I = \begin{bmatrix} C_1 \\ C_2 \\ \vdots \\ C_r \end{bmatrix} = \begin{bmatrix} \{G_1^1, G_2^1, \ldots, G_{n_1}^1\} \\ \{G_1^2, G_2^2, \ldots, G_{n_2}^2\} \\ \vdots \\ \{G_1^r, G_2^r, \ldots, G_{n_r}^r\} \end{bmatrix}. \qquad (8)$$
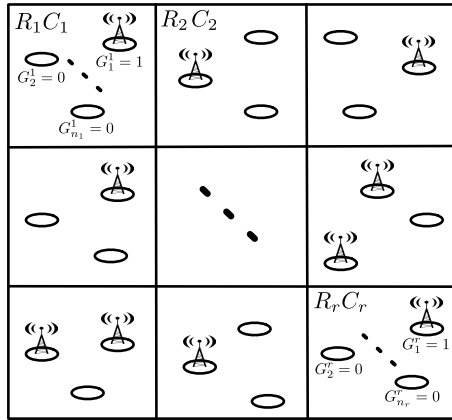
**FIGURE 2. Illustrations of the sub-division and the chromosome segments.**

Note that an individual contains all non-repetitive genes due to the mutual exclusion of the chromosomes segments. Actually, the gene set $\{G_1^1, \ldots, G_{n_1}^1, \ldots, G_1^r, \ldots, G_{n_r}^r\}$ is exactly identical to the gene set $\{G_1, G_2, \ldots, G_n\}$. For the sake of simplicity, we can reorder the sequence of the genes to ensure $G_1 = G_1^1, G_2 = G_2^1, \ldots, G_{n-1} = G_{n_r-1}^r, G_n = G_{n_r}^r$. In the same order, we also reorder the sequence of the candidate sites as $S_1 = S_1^1, S_2 = S_2^1, \ldots, S_{n-1} = S_{n_r-1}^r, S_n = S_{n_r}^r$, and so forth for other symbols including $\alpha_i$ and $c_i$.

A population refers to a batch of individuals, denoted as $\mathbf{P} = \{I_1, I_2, \ldots, I_L\}$ where $L$ is the number of the individuals. Let the chromosome segment $C_{k,l}$ of individual $I_l$ be $C_{k,l} = \{G_1^{k,l}, G_2^{k,l}, \ldots, G_{n_k}^{k,l}\}$. Thus the individual $I_l$ can be described as

$$I_l = \begin{bmatrix} C_{1,l} \\ C_{2,l} \\ \vdots \\ C_{r,l} \end{bmatrix} = \begin{bmatrix} \{G_1^{1,l}, \ldots, G_{n_1}^{1,l}\} \\ \{G_1^{2,l}, \ldots, G_{n_2}^{2,l}\} \\ \vdots \\ \{G_1^{r,l}, \ldots, G_{n_r}^{r,l}\} \end{bmatrix}. \quad (9)$$

### B. FITNESS FUNCTION

We present fitness functions to evaluate the performance of the individual $I_l$ and the chromosome segment $C_{k,l}$. Let the covered region $Cover(I_l)$ of the individual $I_l$ denote the $Cover(\boldsymbol{\alpha}_l)$ in which the parameter $\boldsymbol{\alpha}_l$ corresponds to the selected candidate site subset $\hat{\mathbf{S}}_l$ represented by the chromosome segment of $I_l$, given by

$$\hat{\mathbf{S}}_l = \{S_i^k | G_i^{k,l} = 1, 1 \leq i_k \leq n_k, 1 \leq k \leq r\}. \quad (10)$$

A larger $Cover(I_l)$ means a better global performance of the individual $I_l$.

For a given sub-region $R_k$ and a given individual $I_l$, let $c_i^k(\boldsymbol{\alpha}_l)$ be the covered region of the BS on the candidate site $S_i^k$ if $\alpha_i^{k,l} = 1$, or let $c_i^k(\boldsymbol{\alpha}_l^k) = \varnothing$ if the candidate site $S_i^{k,l}$ is not selected to place a BS, where $1 \leq i \leq n_k$. Now the local
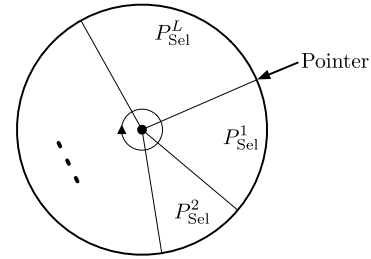


**FIGURE 3. Illustration of the roulette wheel in selection operation.**

coverage area inside the region $R_k$ can be expressed as

$$Cover^k(C_{k,l}) = R_k \cap \left( \sum_{i=1}^{n_k} c_i^k(\boldsymbol{\alpha}_l) \right). \quad (11)$$

A larger $Cover^k(C_{k,l})$ means a better local performance of the individual $I_l$ inside $R_k$.

Denote the fitness function of individual $I_l$ as

$$F_l = (a \cdot |Cover(I_l)|)^b \quad (12)$$

where $|X|$ is the area of the region $X$; $a$ and $b$ are the positive multiplier and the positive exponent to enlarge or reduce the influence of the covered region. Obviously, a larger fitness function $F_l$ leads to a larger covered region and a better performance of individual $I_l$.

Similarly, the fitness function of chromosome segment $C_{k,l}$ can be calculated by

$$F_{k,l} = \left( a \cdot |Cover^k(C_{k,l})| \right)^b. \quad (13)$$

Obviously, a better $C_{k,l}$ in individual $I_l$ has a larger fitness function $F_{k,l}$ as for the sub-region $R_k$.

### C. SELECTION, MUTATION AND CROSSOVER

Selection operation is to select outstanding individuals who usually have high fitness function from a population, so as to breed a new population. Such operation fully reflects the nature rule "survival of the fittest", and the "fittest" individuals will pass on more genes to the next generation, which helps improve the overall performance of the population.

There are various selection methods to breed a new population, such as the roulette wheel selection, the linear ranking selection, the exponential ranking selection and the tournament selection [39]. Here, we adopt the roulette wheel selection. Denote the selection probability of individual $I_l$ as

$$P_{\text{Sel}}^l = \frac{F_l}{\sum\limits_{\hat{l}=1}^{L} F_{\hat{l}}}. \quad (14)$$

Note that the summation of all selection probabilities satisfies

$$\sum_{l=1}^{L} P_{\text{Sel}}^l = 1. \quad (15)$$

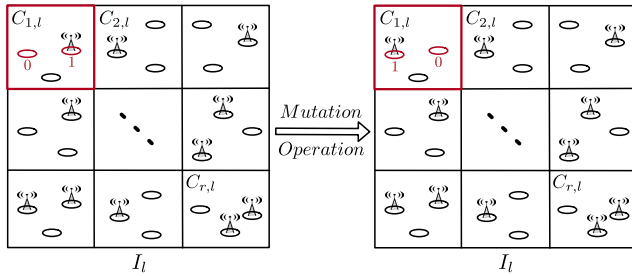The roulette wheel selection is illustrated in Fig. 3.

**FIGURE 4.** Illustration of the mutation operation for individual $I_l$.

Now let us spin the imaginary wheel, and when the roulette stops, the individual corresponding to the sector on which the pointer points is selected to be one of the new population. Do the aforementioned steps repeatedly before the number of the individuals in the new population reaches $L$.

Mutation operation, one of the key operations to maintain genetic diversity, alters one or more genes of individuals from their initial states. Let the mutation probability be $P_{\mathrm{Mut}}$, and then the mutation operation can be conducted according to the following steps:

1) In terms of each individual, randomly generate a number $u$ ranging in $[0, 1]$. If $u \leq P_{\mathrm{Mut}}$, the mutation operation is conducted.
2) Mutation operation: select $N_M$ chromosome segments with the lowest fitness functions of chromosome segment.
3) For each selected chromosome segment, randomly select a gene whose value is 1, and assign its value to 0. Meanwhile, randomly select a gene whose value is 0, and assign its value to 1.

The illustration of the mutation operation for individual $I_l$ is shown in Fig. 4.

Crossover operation refers to combining the genes of two parents, i.e., two individuals, in original population to generate new offspring, i.e., new individuals, in next generation, which increases the probability of jumping out of the local optimal solution due to the randomness. Let the crossover probability be $P_{\mathrm{Cro}}$, and then the crossover operation can be conducted according to the following steps:

1) Divide $L$ individuals into $\frac{L}{2}$ (if $L$ is even) or $\frac{L-1}{2}$ (if $L$ is odd) groups to generate individual pairs.
2) For each individual pair, randomly generate a decimal number $n$ ranging in $[0, 1]$. If $n \leq P_{\mathrm{Cro}}$, conduct the crossover operation. Otherwise, test the next individual pair.
3) Crossover operation: for each chromosome segment in individual pair $(I_p, I_q)$, if $\sum_{i_k=1}^{n_k} G_{i_k}^{k,p} = \sum_{i_k=1}^{n_k} G_{i_k}^{k,q}$, exchange the chromosome segment $C_{k,p}$ of individual $I_p$ and the chromosome segment $C_{k,q}$ of individual $I_q$.

Note that the selected BS sites increases in the optimization process. And the numbers of the selected sites in the same sub-rectangle for individual pairs becomes more and more,

which helps increase the chance to conduce the crossover operation. The illustration of the crossover operation for individual pair $(I_p, I_q)$ is depicted in Fig. 5
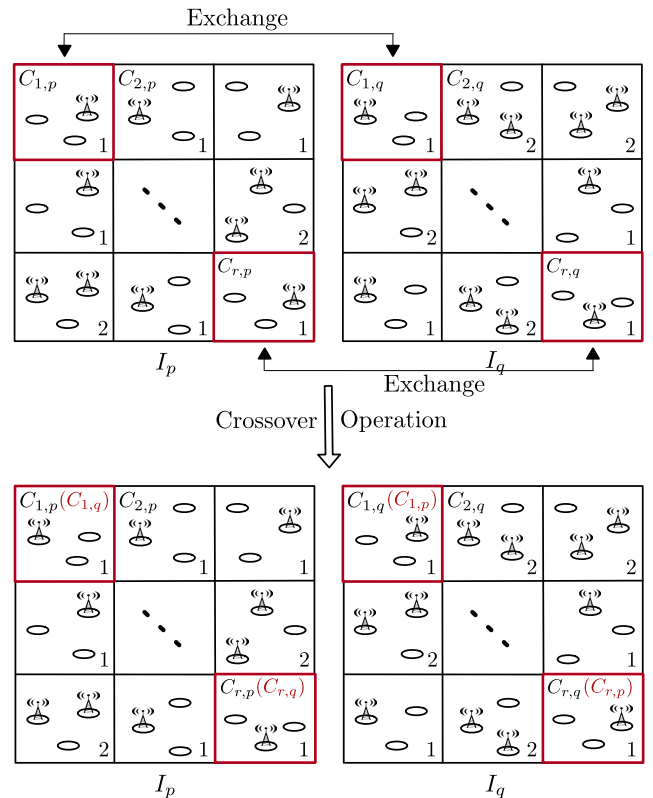


**FIGURE 5.** Illustration of the crossover operation for individual pair $(I_p, I_q)$.

In order to ensure $\sum_{i=1}^{n} G_i = m$, only chromosome segments with the same numbers of selected BS sites can be exchanged in individual pairs. Different from the canonical GA, the exchanged unit is the geometry-induced chromosome segment in crossover operation, which will not destroy the coverage characteristic inside the corresponding sub-region.

Above all, we propose the GGA approach to handle the BS placement problems in wireless cellular networks, as shown in Algorithm 1.

In the canonical GA, the genes in individuals are not in order, which ignores the geometric correlation among the adjacent BSs. Inspired by the preservation of geometric correlation, we design the geometry-induced chromosome segments. With the guidance of the fitness functions of chromosome segments, the mutation operation tends to improve the poor chromosome segments and then the crossover operation remains the segments of chromosomes as far as possible. Different from the canonical GA, the proposed algorithm improves the overall quality of the population not only by the selection operation but also by steadily mutating the poor chromosome segments. Thus, the improved GGA with the

---

**Algorithm 1** Geometry-Induced Genetic Algorithm

**Input:** $\mathbf{S}, n, m, r, L, a, b, P_{\text{Cro}}, P_{\text{Mut}}, N_M$

**Output:** $\alpha, \hat{\mathbf{S}}$

1: Initialize the population $\mathbf{P}$.
2: **while** the number of the generations do not reach the maximum **do**
3:      Calculate $F_l$, $1 \leq l \leq L$.
4:      $\mathbf{P}_{\text{New}} \leftarrow \{\}$
5:      $N_{\text{New}} \leftarrow 0$
6:      Calculate $F_1, F_2, \ldots, F_L$.
7:      Calculate $P^1_{\text{Sel}}, \ldots, P^L_{\text{Sel}}$.
8:      **while** $N_{\text{New}} < L$ **do**
9:          Calculate the index $l$ based on the roulette wheel selection algorithm according to $P^1_{\text{Sel}}, \ldots, P^L_{\text{Sel}}$ in Algorithm 2.
10:          Add individual $I_l$ to set $\mathbf{P}^{\text{New}}$.
11:          $N_{\text{New}} \leftarrow N_{\text{New}} + 1$
12:      **end while**
13:      $\mathbf{P} \leftarrow \mathbf{P}_{\text{New}}$
14:      Conduct the mutation operation in Algorithm 3.
15:      Conduct the crossover operation in Algorithm 4.
16: **end while**
17: $I \leftarrow \arg\max\limits_{I_l} Cover(I_l)$
18: Realign the index $i$ according to the sequence of the gene set $\{G^1_1, \ldots, G^1_{n_1}, \ldots, G^r_1, \ldots, G^r_{n_r}\}$.
19: $\alpha \leftarrow G$
20: $\hat{\mathbf{S}} \leftarrow \{S_i | \alpha_i = 1, 1 \leq i \leq n\}$

---

**Algorithm 2** Roulette-Wheel Selection Algorithm

**Input:** $P_1, P_2, \ldots, P_N$

**Output:** *index*

1: Randomly select a decimal $0 \leq n \leq 1$.
2: $n_{\text{sum}} \leftarrow 0$
3: **for** $i \leftarrow 1, N$ **do**
4:      $n_{\text{sum}} \leftarrow n_{\text{sum}} + P_i$
5:      **if** $n \leq n_{\text{sum}}$ **then**
6:          $index \leftarrow i$
7:          **break**
8:      **end if**
9: **end for**

---

**Algorithm 3** Mutation Operation

**Input:** $\mathbf{P}, r, L, P_{Mut}, N_M$

**Output:** $\mathbf{P}$

1: Calculate $F_{k,l}$, $1 \leq k \leq r$, $1 \leq l \leq L$ in $\mathbf{P}$.
2: **for** $l \leftarrow 1, L$ **do**
3:      Randomly generate $0 \leq n \leq 1$.
4:      **if** $n \leq P_{\text{Mut}}$ **then**
5:          Calculate $F_{1,l}, \ldots, F_{r,l}$.
6:          Calculate $P^{1,l}_{\text{Mut}}, \ldots, P^{r,l}_{\text{Mut}}$.
7:          Select $N_M$ chromosome segments with the lowest fitness functions of chromosome segment.
8:          **for** $\hat{k} \leftarrow 1, N_M$ **do**
9:              Randomly select a gene $G^{\hat{k},l}_p = 1$.
10:              $G^{\hat{k},l}_p \leftarrow 0$
11:              Randomly select a gene $G^{\hat{k},l}_q = 0$.
12:              $G^{\hat{k},l}_q \leftarrow 1$
13:          **end for**
14:      **end if**
15: **end for**

---

**Algorithm 4** Crossover Operation

**Input:** $\mathbf{P}, r, L, P_{Cro}$

**Output:** $\mathbf{P}$

1: Divide $L$ individuals in $\mathbf{P}$ into $N_G$ pairs.
2: **for** $\hat{l} \leftarrow 1, N_G$ **do**
3:      Randomly generate $0 \leq n \leq 1$.
4:      **if** $n \leq P_{\text{Cro}}$ **then**
5:          **for** $k \leftarrow 1, r$ **do**
6:              **if** $\sum\limits_{i_k=1}^{n_k} G^{k,p}_{i_k} = \sum\limits_{i_k=1}^{n_k} G^{k,q}_{i_k}$ **then**
7:                  Exchange $C_{k,p}$ and $C_{k,q}$.
8:              **end if**
9:          **end for**
10:      **end if**
11: **end for**

---

extra guidance possibly helps accelerate the optimization process compared with the canonical GA.

## V. EXPERIMENTS WITH IDEAL DISK BS COVERAGE MODEL

In this section, we first introduce the simulation scenario and propose the ideal disk coverage model for BSs. Then, we describe the process of deciding the hyper-parameters. Finally, we prove the feasibility and the efficiency of the GGA by comparing it with the canonical GA.

### A. SIMULATION SCENARIO MODELING

Experiments are done in an $L_{\text{Ideal}} \times L_{\text{Ideal}}$ region. According to the ideal honeycomb shape, we first add $m$ locations, $S_1, S_2, \ldots, S_m$, which distributed at the centers of the hexagons, into the candidate site set, as shown in Fig. 6.

Then, we randomly add $n - m$ locations inside the ROI, $S_{m+1}, S_{m+2}, \ldots, S_n$, into the candidate site set. We also assume that the ROI is flat, where the elevation $H_{\text{ele}}$ for any locations is always 0m. The settings of parameters are listed in Table 2.

We adopt the ideal disk coverage model, in which the maximum covered region of a single BS, say $S$, is the intersection of a disk with center at $S$ and radius of $r_c$. If a given location $p$ is covered by two or more BSs, it will select the nearest BS, or one among the nearest BSs if there exist two or more BSs with the same shortest distance away from it, to access the
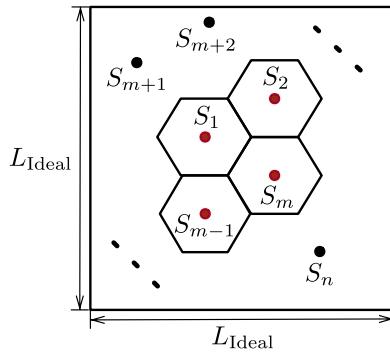
**FIGURE 6.** Illustration of the simulation scenario.

**TABLE 2.** Settings of parameters.

| Parameter | Value |
|---|---|
| $L_{Ideal}$ | 6.25 km |
| $n$ | 600 |
| $m$ | 213 |
| a | 10 |
| b | 2 |
| $N_M$ | 6 |
| $H_{ele}$ | 0m |

mobile network. So any location is covered at most by one BS. The covered region of the BS is really a disk intersected with a cell of the Voronoi diagram [40] determined by all the BSs.

Let $(x_i, y_i)$ denote the coordinate of the candidate site $S_i$. Then, the covered region $c_i$ of $S_i$ is given by

$$c_i(\alpha) = \begin{cases} D_i(x_i, y_i, r_c) \cap V_i(x_i, y_i) & \text{if } \alpha_i \neq 0, \\ 0 & \text{otherwise,} \end{cases} \quad (16)$$

where

$$D_i(x_i, y_i, r_c) = \left\{ (x, y) \mid \sqrt{(x - x_i)^2 + (y - y_i)^2} \leq r_c \right\}, \quad (17)$$

$$V_i(x_i, y_i) = \{(x, y) \mid E_{dist}((x, y), (x_i, y_i)) \leq E_{dist}((x, y), (x_{\hat{i}}, y_{\hat{i}})), 1 \leq \hat{i} \leq n, \hat{i} \neq i\}, \quad (18)$$

$$E_{dist}\left((x_i, y_i), (x_{\hat{i}}, y_{\hat{i}})\right) = \sqrt{(x_i - x_{\hat{i}})^2 + (y_i - y_{\hat{i}})^2}. \quad (19)$$

Without loss of generality, we take $r_c = 0.3km$.

Based on the GGA presented in Algorithm 1, the following simulation experiments are executed on a notebook with an Intel i5 Core running at 1.6GHz. The software environment is Python at version 3.5 and Numpy at version 1.14.2.

### B. HYPER-PARAMETER DECISION

There are four hyper-parameters $L$, $P_{Cro}$, $P_{Mut}$ and $r$ in GGA. The coefficient $L$ is the number of the individuals in population. The crossover probability $P_{Cro}$ indicates how many individual pairs will conduct the crossover operation.

If $P_{Cro}$ is too small, the speed for generating new individuals is too slow to converge to the optimum. On the contrary, if $P_{Cro}$ is too large, the individual with high fitness function will be destroyed with high probability. As for the mutation probability $P_{Mut}$, if it is too small, the probability to generate new characteristics is too small; if it is too large, the GA will be degraded into the random searching algorithm. The coefficient $r$ is the number of the sub-rectangles, i.e., the number of the chromosome segments in an individual, which indicates how much geometric information we can obtain. If $r = 1$, the whole region is regarded as an integration to conduct the crossover operation, and thus such crossover operation is meaningless because no new individuals are generated. Larger $r$ indicates more geometric information, larger probability to conduct crossover operation but larger calculated amount. However, if $r$ is too large, or even $r = n$, that is, each sub-rectangle contains only one candidate BS site, the crossover operation will never be conducted. Therefore, it is essential to choose the optimal or near-optimal hyper-parameters to achieve high convergence rate.

In order to better the performance, we utilize the orthogonal array testing to obtain the near-optimal hyper-parameter settings, listed in Table 3. The four-level values of the hyper-parameters are given in Table 4.

**TABLE 3.** The orthogonal array L16($4^4$) for GGA.

| Experiment No. | $L$ | $P_{Cro}$ | $P_{Mut}$ | $r$ |
|---|---|---|---|---|
| 1 | 1 | 1 | 1 | 1 |
| 2 | 1 | 2 | 2 | 2 |
| 3 | 1 | 3 | 3 | 3 |
| 4 | 1 | 4 | 4 | 4 |
| 5 | 2 | 1 | 2 | 3 |
| 6 | 2 | 2 | 1 | 4 |
| 7 | 2 | 3 | 4 | 1 |
| 8 | 2 | 4 | 3 | 2 |
| 9 | 3 | 1 | 3 | 4 |
| 10 | 3 | 2 | 4 | 3 |
| 11 | 3 | 3 | 1 | 2 |
| 12 | 3 | 4 | 2 | 1 |
| 13 | 4 | 1 | 4 | 2 |
| 14 | 4 | 2 | 3 | 1 |
| 15 | 4 | 3 | 2 | 4 |
| 16 | 4 | 4 | 1 | 3 |

**TABLE 4.** The four-level values of hyper-parameters.

| Level | $L$ | $P_{Cro}$ | $P_{Mut}$ | $r$ |
|---|---|---|---|---|
| 1 | 1 | 0.8 | 0.1 | 1 |
| 2 | 5 | 0.85 | 0.4 | 9 |
| 3 | 10 | 0.9 | 0.7 | 25 |
| 4 | 15 | 0.95 | 1 | 49 |

We adopt the coverage ratio to reflect how large the covered region is, given by

$$C_{Ratio} = \frac{|Cover|}{|R|}. \quad (20)$$

Larger $C_{Ratio}$ indicates larger covered region and better performance.

(a) $L$.

(b) $P_{\text{Cro}}$.
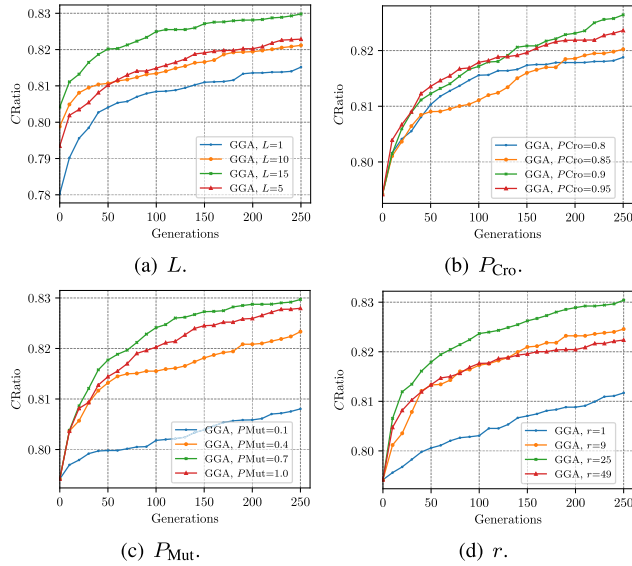
(c) $P_{\text{Mut}}$.

(d) $r$.

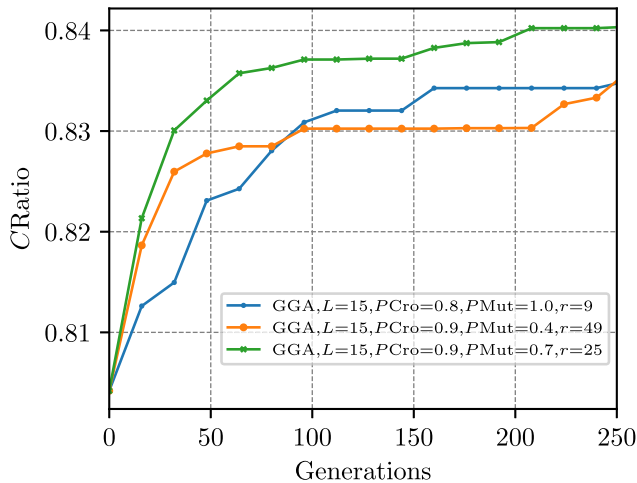**FIGURE 7.** Average Performance of four hyper-parameters.



**FIGURE 8.** Performance comparison of different hyper-parameter settings.

We carry out the 16 experiments in the orthogonal array over 20 Monte Carlo runs. The average performance of four hyper-parameters is illustrated in Fig. 7. The coverage ratio $C_{\text{Ratio}}$ of each generation is the largest one among those in the previous and the corresponding populations.

It can be observed that the optimal hyper-parameters in the orthogonal test are $L = 15$, $P_{\text{Cro}} = 0.9$, $P_{\text{Mut}} = 0.7$ and $r = 25$. Then, we compare the curves with such hyper-parameter settings with the two best curves in 16 orthogonal experiments, shown in Fig. 8.

We select the best curve, and its hyper-parameter settings are shown in Tabel 5.

Thus, we take the hyper-parameters $L = 15$, $P_{\text{Cro}} = 0.9$, $P_{\text{Mut}} = 0.7$ and $r = 25$ in the following experiments.

## C. PERFORMANCE EVALUATION

We first testify the feasibility of the GGA. We randomly generate a population **P** and select the individual with the

**TABLE 5.** The near-optimal hyper-parameter settings in GGA.

| Parameter | Value |
|---|---|
| $L$ | 15 |
| $P_{\text{Cro}}$ | 0.9 |
| $P_{\text{Mut}}$ | 0.7 |
| $r$ | 25 |

highest $C_{\text{Ratio}}$ as the best individual. Similarly, in each generation, we also select the individual with the highest $C_{\text{Ratio}}$ from the corresponding population as the best individual. The illustrations of the coverage maps of the best individuals before and after the GGA optimization are depicted in Fig. 9.
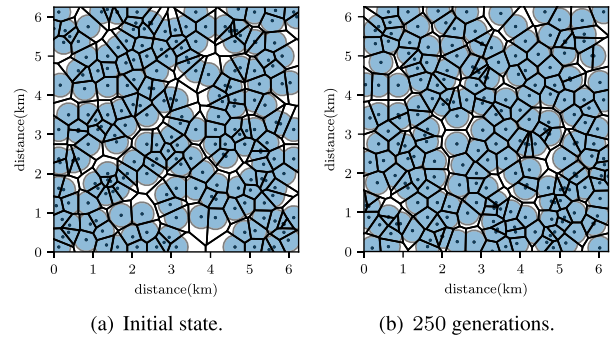


(a) Initial state.

(b) 250 generations.

**FIGURE 9.** Illustrations of the coverage maps of the best individuals before and after the GGA optimization.

The blue regions represent the covered regions, and the white ones represent the uncovered regions. After the GGA optimization, the covered blue regions increase while the uncovered white regions decrease. In addition, the coverage ratio grows from 80.06% to 84.32%. It indicates that the GGA is applicable in dealing with the BS placement problems.

Then, we testify the efficiency from the perspective of the convergence speed. The proposed GGA is an improved version of the canonical GA. Therefore, we utilize the GA to compare the performance. Here, we briefly introduce the algorithm process. Denote the individual in GA as $I_l^{\text{GA}} = \{G_1, \ldots, G_n\}$. Note that the genes in an individual are unordered and not related to the geometric locations of their corresponding BSs. The calculation process of the individual fitness function and the selection operation is as same as that of the the GGA. The mutation operation can be conducted according to the following steps:

1) In terms of each individual, randomly generate a decimal number $n$ ranging in $[0, 1]$. If $n \leq P_{\text{Mut}}$, conduct the Mutation operation.

2) Mutation operation: randomly select $N_M$ genes whose values are 1, and change their values from 1 to 0. Similarly, randomly select $N_M$ genes whose values are 0, and change their values from 0 to 1.

The crossover operation is conducted according to the following steps:

1) Divide $L$ individuals into $\frac{L}{2}$ (if $L$ is even) or $\frac{L-1}{2}$ (if $L$ is odd) groups to generate individual pairs.
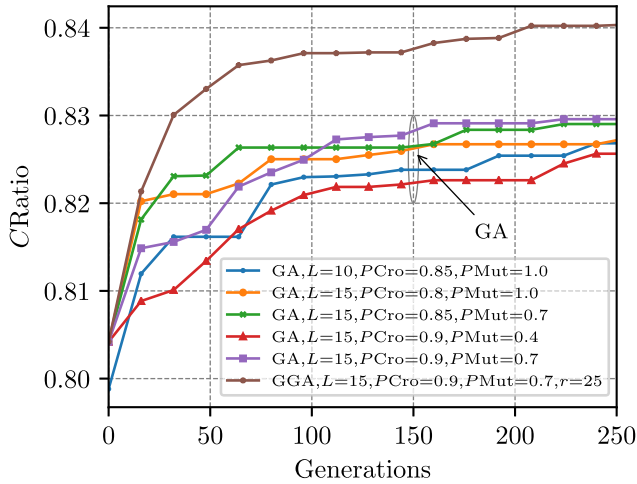
**FIGURE 10.** Illustrations of the coverage ratios versus generations of GGA and GA for 250 generations.

2) For each individual pair, randomly generate a decimal number $n$ ranging in $[0, 1]$. If $n \leq P_{\text{Cro}}$, conduct the crossover operation.

3) Crossover operation: randomly divide the genes in the two individuals into $r$ groups where the gene numbers are the same. For each gene group, if the numbers of genes with "1" values of the individual pair are the same, exchange the gene groups of the two individuals.

Obviously, the canonical GA only utilizes the guidance of the coverage of the whole ROI, which neglects the geometric guidance.

The illustrations of the coverage ratios versus generations of GGA and GA for 250 generations are depicted in Fig. 10.

Since the initial populations are randomly generated, the initial coverage ratios of the GGA and the GA are different under the condition of different $L$. First, the coverage ratios are increasing and tend to a definite value, which implies both GGA and GA are feasible for handling the BS placement problems. Note that we can only obtain the near-optimal or the satisfactory solution of the optimization problem unless the number of the generations is infinity. Second, the convergence speed of the GGA is faster than that of the canonical GA. This is mainly caused by the extra guidance of the geometric information, i.e., the geometry-induced chromosomes.

Above all, the proposed GGA algorithm shows a good performance in handling the BS placement problems in wireless cellular networks.

## VI. EXPERIMENTS WITH REAL RADIO SIGNAL BS COVERAGE MODEL

In this section, we first present the real radio signal BS coverage model. Then, we testify the applicability and the efficiency of the GGA.

### A. SIMULATION SCENARIO AND BS COVERAGE MODEL

Experiments are done in the same ROI modeled in Section V-A. All the parameters listed in Table 2 are not changed. Each BS prepared to be installed in the ROI has three antennas. The azimuths of three antennas in each BS are assigned to an equal difference series, say, $0°$, $120°$ and $240°$, in order to create non-overlapping $360°$ coverage from this BS. All tilts of antennas are chosen as $8°$. Assume that all cells are fully loaded.

Assume that the covered region of a single BS is the region where the signal strength and the signal quality both satisfy the requirements. For an arbitrary coordinate $(x, y)$ in the ROI, RSRP refers to as the Reference Signal Received Power among all the signal powers from antennas, indicating the maximal signal strength, given by

$$P^{\text{RS}}(x, y) = \max_{j \in \mathbf{J}} P_j(x, y) \qquad (21)$$

where $\mathbf{J} = \{1, \ldots, 3m\}$ is the set of the antenna indexes. The variable $P_j^{\text{SI}}$ is the signal power on coordinate $(x, y)$ from the $j$-th antenna, described as

$$P_j(x, y) = P_{\text{tx}} + Gain_j(x, y) + G_{\text{terminal}} \\ - PL_j(x, y) - \sigma_{\text{S}} \qquad (22)$$

where $P_{\text{tx}}$ is the transmit power; $Gain_j$ is the directional antenna gain from $j$-th antenna to coordinate $(x, y)$; $G_{\text{terminal}}$ is the mobile terminal antenna gain; $PL_j$ is the path loss from $j$-th antenna to coordinate $(x, y)$ and here we use the COST231-Hata model [41] ; $\sigma_{\text{S}}$ is the shadow fading margin. SINR is denoted as the Ratio of received useful Signal power to the Interferences plus the Noise power, indicating the signal quality, computed as

$$P^{\text{SI}}(x, y) = 10 \log_{10} \frac{P^{\text{RS}}(x, y)}{N_{\text{Noise}} + \sum_{\substack{j \in J \\ j \neq \hat{j}(x, y)}} P_j(x, y)}, \qquad (23)$$

$$\hat{j}(x, y) = \arg \max_{j \in \mathbf{J}} P_j(x, y) \qquad (24)$$

where $N_{\text{Noise}}$ is the power of the noise.

Denote the three antennas installed on BS candidate site $S_i$ as $a_1^i$, $a_2^i$ and $a_3^i$. Then, the BS covered region $c_i$ is expressed as

$$c_i(\boldsymbol{\alpha}) = \begin{cases} \sum_{j=1}^{3} H(a_j^i) & \text{if } \alpha_i \neq 0, \\ 0 & \text{otherwise,} \end{cases} \qquad (25)$$

$$H(a_j^i) = \{(x, y) | P^{\text{RS}}(x, y) \geq \text{TH}_{\text{RS}} \text{ and} \\ \times P^{\text{SI}}(x, y) \geq \text{TH}_{\text{SI}} \text{ and } \hat{j}(x, y) = j\} \qquad (26)$$

where $\text{TH}_{\text{RS}}$ and $\text{TH}_{\text{SI}}$ are the thresholds of RSRP and SINR, respectively.

Other settings of parameters are listed in Table 6

The hyper-parameters $L$, $P_{\text{Pro}}$, $P_{\text{Mut}}$ and $r$ are assigned to $5$, $0.8$, $0.4$ and $25$ according to the orthogonal test as what has been discussed above.
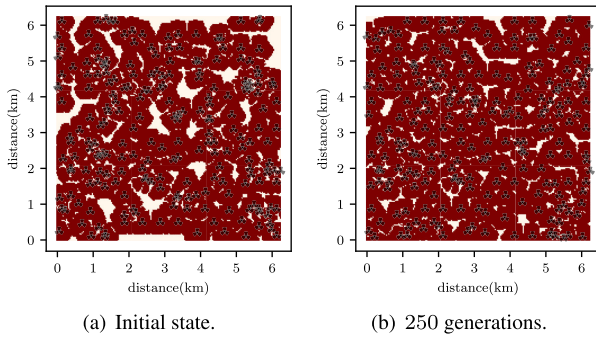
(a) Initial state.  (b) 250 generations.

**FIGURE 11.** Illustrations of the coverage maps of the best individuals before and after the GGA optimization.

**TABLE 6.** Settings of parameters.

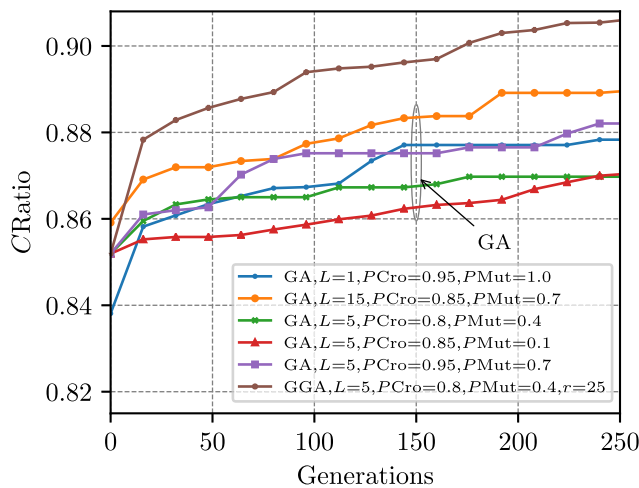| Parameter | Value |
|---|---|
| $G_{terminal}$ | 2 dB |
| $\sigma_S$ | 7.25 dB |
| $P_{tx}$ | 24 dB |
| $TH_{RS}$ | −100 dBm |
| $TH_{SI}$ | −3 dB |
| $N_{Noise}$ | -110 dB |



**FIGURE 12.** Illustrations of the coverage ratios versus generations of GGA and GA for 250 generations.

### B. PERFORMANCE EVALUATION

First, we prove the applicability of the GGA. The illustrations of the coverage maps of the best individuals before and after the GGA optimization are depicted in Fig. 11. The red regions represent the covered regions, and the white ones represent the uncovered regions. After the GGA optimization, the coverage ratio is improved to 91.73% from 85.23%. Therefore, the GGA is applicable for handling the BS placement problems.

The illustrations of the coverage ratios versus generations of GGA and GA for 250 generations are depicted in Fig. 12.

The shapes and the trends of the curves in the experiments with real radio signal BS coverage model are as same as those in the experiments with ideal disk BS coverage model. It is

obvious that the efficiency of the GGA is higher than that of the canonical GA.

In summary, with the guidance of the geometry-induced chromosome segments, the proposed GGA handles the BS placement problems in an efficient manner.

## VII. CONCLUSION

It is important to handle the BS placement problems accurately and efficiently during the BS deployment phase. By taking the geometric correlation among BSs into consideration, we propose a novel GGA as an efficient treatment to facilitate BS placement problems in wireless cellular networks.

We design the experiments in an ideal scenario where the expected optimal subset of the candidate sites is known previously. The experiment results reach the expectation. Moreover, the GGA performs well in handling the BS placement problems and is more efficient than the canonical GA. The same conclusion holds for the real scenario. Consequently, with the geometry-induced chromosome segments, the proposed GGA is suitably applied to the BS placement problems in the cellular networks.

### REFERENCES

[1] M. Bennis, M. Debbah, and H. V. Poor, "Ultrareliable and low-latency wireless communication: Tail, risk, and scale," *Proc. IEEE*, vol. 106, no. 10, pp. 1834–1853, Oct. 2018.

[2] T. Sanguanpuak, S. Guruacharya, E. Hossain, N. Rajatheva, and M. Latva-aho, "Infrastructure sharing for mobile network operators: Analysis of trade-offs and market," *IEEE Trans. Mobile Comput.*, vol. 17, no. 12, pp. 2804–2817, Dec. 2018.

[3] S. Wang and C. Ran, "Rethinking cellular network planning and optimization," *IEEE Wireless Commun.*, vol. 23, no. 2, pp. 118–125, Apr. 2016.

[4] S. Sekander, H. Tabassum, and E. Hossain, "Multi-tier drone architecture for 5G/B5G cellular networks: Challenges, trends, and prospects," *IEEE Commun. Mag.*, vol. 56, no. 3, pp. 96–103, Mar. 2018.

[5] C. T. Cicek, H. Gultekin, B. Tavli, and H. Yanikomeroglu, "UAV base station location optimization for next generation wireless networks: Overview and future research directions," in *Proc. 1st Int. Conf. Unmanned Vehicle Syst.-Oman (UVS)*, Feb. 2019, pp. 1–6.

[6] G. K. Audhya, K. Sinha, P. Majumder, S. R. Das, and B. P. Sinha, "Placement of access points in an ultra-dense 5G network with optimum power and bandwidth," in *Proc. IEEE Wireless Commun. Netw. Conf. (WCNC)*, Apr. 2018, pp. 1–6.

[7] P. Calégari, F. Guidec, and P. Kuonen, "A parallel genetic approach to transceiver placement optimisation," in *Proc. Parallel Distrib. Syst. Work.*, 1996, pp. 21–24.

[8] B. Chamaret, S. Josselin, P. Kuonen, M. Pizarroso, B. Salas-Manzanedo, S. Ubeda, and D. Wagner, "Radio network optimization with maximum independent set search," in *Proc. IEEE 47th Veh. Technol. Conf. Technol. Motion*, May 1997, pp. 770–774.

[9] F. Lagum, S. S. Szyszkowicz, and H. Yanikomeroglu, "CoV-based metrics for quantifying the regularity of hard-core point processes for modeling base station locations," *IEEE Wireless Commun. Lett.*, vol. 5, no. 3, pp. 276–279, Jun. 2016.

[10] S. Arora, "Approximation schemes for NP-hard geometric optimization problems: A survey," *Math. Program.*, vol. 97, no. 1, pp. 43–69, Jul. 2003.

[11] Y. Yang, W. Yi, T. Zhang, G. Cui, L. Kong, X. Yang, and J. Yang, "Fast optimal antenna placement for distributed MIMO radar with surveillance performance," *IEEE Signal Process. Lett.*, vol. 22, no. 11, pp. 1955–1959, Nov. 2015.

[12] A. Gupta and E. R. K. Jha, "A survey of 5G network: Architecture and emerging technologies," *IEEE Access*, vol. 3, pp. 1206–1232, 2015.

[13] Z. A. El Moiz Dahi, C. Mezioud, and A. Draa, "On the efficiency of the binary flower pollination algorithm: Application on the antenna positioning problem," *Appl. Soft Comput.*, vol. 47, pp. 395–414, Oct. 2016.

[14] M. Agiwal, A. Roy, and N. Saxena, "Next generation 5G wireless networks: A comprehensive survey," *IEEE Commun. Surveys Tuts.*, vol. 18, no. 3, pp. 1617–1655, 3rd Quart., 2016.

[15] D. Whitley, "A genetic algorithm tutorial," *Statist. Comput.*, vol. 4, no. 2, pp. 65–85, Jun. 1994.

[16] S. Lee, S. Lee, K. Kim, and Y. H. Kim, "Base station placement algorithm for large-scale LTE heterogeneous networks," *PLoS ONE*, vol. 10, no. 10, Oct. 2015, Art. no. e0139190.

[17] S.-K. Gupta, P. Kuila, and P. K. Jana, "Genetic algorithm approach for *k*-coverage and *m*-connected node placement in target based wireless sensor networks," *Comput. Elect. Eng.*, vol. 56, pp. 544–556, Nov. 2016.

[18] Y. Chen, N. Li, C. Wang, W. Xie, and J. Xv, "A 3D placement of unmanned aerial vehicle base station based on multi-population genetic algorithm for maximizing users with different QoS requirements," in *Proc. IEEE 18th Int. Conf. Commun. Technol. (ICCT)*, Oct. 2018, pp. 967–972.

[19] M. H. Wright, "Optimization methods for base station placement in wireless applications," in *Proc. 48th IEEE Veh. Technol. Conf. Pathway Global Wireless Revolution*, May 1998, pp. 387–391.

[20] M. Radmard, M. M. Chitgarha, M. N. Majd, and M. M. Nayebi, "Antenna placement and power allocation optimization in MIMO detection," *IEEE Trans. Aerosp. Electron. Syst.*, vol. 50, no. 2, pp. 1468–1478, Apr. 2014.

[21] O. Abdelkhalek, H. Masri, and S. Krichen, "An adaptive variable neighborhood search for solving the multi-objective node placement problem," *Electron. Notes Discrete Math.*, vol. 47, pp. 189–196, Feb. 2015.

[22] S. Bi and R. Zhang, "Node placement optimization in wireless powered communication networks," in *Proc. IEEE Global Commun. Conf. (GLOBECOM)*, Dec. 2015, pp. 1–6.

[23] F. Lagum, I. Bor-Yaliniz, and H. Yanikomeroglu, "Strategic densification with UAV-BSs in cellular networks," *IEEE Wireless Commun. Lett.*, vol. 7, no. 3, pp. 384–387, Jun. 2017.

[24] J. Kennedy and R. C. Eberhart, "A discrete binary version of the particle swarm algorithm," in *Proc. IEEE Int. Conf. Syst., Man, Cybern. Comput. Cybern. Simulation*, Oct. 2007, pp. 4104–4108.

[25] M. H. Kashan, N. Nahavandi, and A. H. Kashan, "DisABC: A new artificial bee colony algorithm for binary optimization," *Appl. Soft Comput.*, vol. 12, no. 1, pp. 342–352, Jan. 2012.

[26] D. Rodrigues, L. A. M. Pereira, T. N. S. Almeida, J. P. Papa, A. N. Souza, C. C. O. Ramos, and X.-S. Yang, "BCS: A binary cuckoo search algorithm for feature selection," in *Proc. IEEE Int. Symp. Circuits Syst.*, May 2013, pp. 465–468.

[27] A. Al-Samawi, A. Sali, N. K. Noordin, M. Othman, and F. Hashim, "Base station location optimisation in LTE using genetic algorithm," in *Proc. Int. Conf. ICT Converg. (ICTC)*, Oct. 2013, pp. 336–341.

[28] X. Huang, U. Behr, and W. Wiesbeck, "Automatic base station placement and dimensioning for mobile network planning," in *Proc. 52nd Veh. Technol. Conf.*, Sep. 2000, pp. 1544–1549.

[29] J. Hu and E. Goodman, "Wireless access point configuration by genetic programming," in *Proc. Congr. Evol. Comput.*, Jun. 2004, pp. 1178–1184.

[30] J. Munyaneza, A. Kurien, and B. Van Wyk, "Optimization of antenna placement in 3G networks using genetic algorithms," in *Proc. 3rd Int. Conf. Broadband Commun. Inf. Technol. Biomed. Appl.*, Nov. 2008, pp. 30–37.

[31] L. Raisanen and R. M. Whitaker, "Comparison and evaluation of multiple objective genetic algorithms for the antenna placement problem," *Mobile Netw. Appl.*, vol. 10, nos. 1–2, pp. 79–88, Feb. 2005.

[32] C.-K. Ting, C.-N. Lee, H.-C. Chang, and J.-S. Wu, "Wireless heterogeneous transmitter placement using multiobjective variable-length genetic algorithm," *IEEE Trans. Syst., Man, Cybern., B, (Cybern.)*, vol. 39, no. 4, pp. 945–958, Apr. 2009.

[33] O. Abdelkhalek, S. Krichen, and A. Guitouni, "A genetic algorithm based decision support system for the multi-objective node placement problem in next wireless generation network," *Appl. Soft Comput.*, vol. 33, pp. 278–291, Aug. 2015.

[34] C. Maple, L. Guo, and J. Zhang, "Parallel genetic algorithms for third generation mobile network planning," in *Proc. Parallel Comput. Elect. Eng. Int. Conf.*, Sep. 2004, pp. 229–236.

[35] J. K. Han, B. S. Park, Y. S. Choi, and H. K. Park, "Genetic approach with a new representation for base station placement in mobile communications," in *Proc. IEEE 54th Veh. Technol. Conf. VTC*, Oct. 2001, pp. 2703–2707.

[36] J.-Y. Wang, J.-B. Wang, and M. Chen, "System capacity analysis and antenna placement optimization for downlink transmission in distributed antenna systems," *Wireless Pers. Commun.*, vol. 71, no. 1, pp. 531–554, Sep. 2013.

[37] C. Yang, X. Zhang, X. Huang, Z. Cheng, X. Zhang, and X. Hou, "Optimal sensor placement for deployable antenna module health monitoring in SSPS using genetic algorithm," *Acta Astronautica*, vol. 140, pp. 213–224, Nov. 2017.

[38] Z. A. El M. Dahi, C. Mezioud, and A. Draa, "A quantum-inspired genetic algorithm for solving the antenna positioning problem," *Swarm Evol. Comput.*, vol. 31, pp. 24–63, Dec. 2016.

[39] A. Shukla, H. M. Pandey, and D. Mehrotra, "Comparative review of selection techniques in genetic algorithm," in *Proc. Int. Conf. Futuristic Trends Comput. Anal. Knowl. Manage. (ABLAZE)*, 2015, pp. 515–519.

[40] F. Aurenhammer, "Voronoi diagrams—A survey of a fundamental geometric data structure," *ACM Comput. Surv.*, vol. 23, no. 3, pp. 345–405, Sep. 1991.

[41] V. S. Abhayawardhana, I. J. Wassell, D. Crosby, M. P. Sellars, and M. G. Brown, "Comparison of empirical propagation path loss models for fixed wireless access systems," in *Proc. IEEE 61st Veh. Technol. Conf.*, May/Jun. 2005, pp. 73–77.

**YAXI LIU** received the B.S. degree from the School of Computer and Communication Engineering, University of Science and Technology Beijing (USTB), Beijing, China, in 2012, where she is currently pursuing the Ph.D. degree. Her research interests include network planning, network optimization, wireless cellular networks, the Internet of Things, and wireless sensor networks.

**WEI HUANGFU** received the M.S. and Ph.D. degrees in electronic engineering from Tsinghua University, Beijing, China, in 1998 and 2001, respectively. He is currently an Associate Professor with the School of Computer and Communication Engineering, University of Science and Technology Beijing (USTB). His main research interests include statistical signal processing, cooperative communications networks, the Internet of Things, and wireless sensor networks.

**HAIJUN ZHANG** (M'13–SM'17) was a Postdoctoral Research Fellow with the Department of Electrical and Computer Engineering, The University of British Columbia (UBC), Canada. He is currently a Full Professor with the University of Science and Technology Beijing, China. He received the IEEE CSIM Technical Committee Best Journal Paper Award, in 2018, and the IEEE ComSoc Young Author Best Paper Award, in 2017. He serves as an Editor of the IEEE Transactions on Communications, the IEEE Transactions on Green Communications Networking, and the IEEE Communications Letters.

**HAOBIN WANG** received the M.S. degree from the School of Computer and Communication Engineering, University of Science and Technology Beijing (UTSB), Beijing, China, in 2019. He is currently with the China Telecom Beijing Research Institute (CTBRI), China Telecom Company Ltd. His research interests include network planning, network optimization, and artificial intelligence.

**WEI AN** received the B.S. degree from the School of Communication Engineering, Shenyang University of Technology (SUT), Shenyang, China, in 2017. He is currently pursuing the M.S. degree with the University of Science and Technology Beijing. His research interests include network planning, network optimization, and machine learning.

**KEPING LONG** received the M.S. and Ph.D. degrees in electric circuit and systematic from the University of Electronic Science and Technology of China (UESTC), Chengdu, China, in 1995 and 1998, respectively. He is currently a Professor with the School of Computer and Communication Engineering, University of Science and Technology Beijing (USTB). His main research interests include statistical signal processing, channel estimation in multiple-input multiple-output (MIMO) orthogonal frequency division multiplexing (OFDM) systems, cooperative communications, and computer networks.

● ● ●